SoftwareX 12 (2020) 100594

Contents lists available at ScienceDirect

SoftwareX

journal homepage: www.elsevier.com/locate/softx

Original software publication

StimVis: A tool for interactive computation of the TMS-induced effects over tractography data

Sofya Kulikova

National Research University Higher School of Economics, Perm, Russia

ARTICLE INFO

Article history:
Received 26 March 2020
Received in revised form 4 September 2020
Accepted 15 September 2020

Keywords:
Transcranial magnetic stimulation
Effective field
Diffusion-weighted imaging
Modeling
Visualization

ABSTRACT

Transcranial magnetic stimulation (TMS) is a promising diagnostic and therapeutic approach. TMS effects depend on multiple technical and individual factors, including anatomical variability. The latter may become particularly important in pathological conditions and contribute to the ambiguity in the results from clinical trials and meta-analyses. Theoretical studies suggest that TMS effects strongly depend on the local orientation of the stimulated fibers. However, these models remain unconfirmed by experimental studies, since current modeling tools compute the induced and not the effective electric field. Here we propose a tool, incorporating information on fiber orientation into TMS effects modeling. This tool may be useful for relating the theoretical mechanisms to the experimentally observed TMS effects and for future development of the personalized TMS approaches.

Code metadata

Current code version	v0.1.2
Permanent link to code/repository used for this code version	https://github.com/ElsevierSoftwareX/SOFTX_2020_146
Code Ocean compute capsule	https://codeocean.com/capsule/4831833/tree/v1
Legal Code License	BSD-3-Clause
Code versioning system used	git
Software code languages, tools, and services used	Python
Compilation requirements, operating environments & dependencies	Python packages: numpy, dipy, fury, vtkplotter, matplotlib; SimNIBS; OpenGL drivers
If available Link to developer documentation/manual	
Support email for questions	SPKulikova@hse.ru

1. Motivation and significance

Transcranial magnetic stimulation (TMS) is a promising non-invasive technique for both diagnostics and treatment of various neurological and psychiatric conditions [1]. Depending on the stimulation settings, TMS may have both inhibitory and excitatory effects on various neuronal populations via different neuronal mechanisms [2,3]. Apart from the technical factors, TMS effects also depend on individual's characteristics, such as age, gender, and anatomical variability [4–6]. The latter may become particularly important in pathological conditions [7–9] and, at least partially, may account for the ambiguity in the results from clinical trials and meta-analyses [8,10–12].

Theoretical models suggest that TMS-induced effects should depend on the co-called effective electrical field, i.e. projection of the induced electrical field E_l to the local orientation of the stimulated axons [13,14]. Furthermore, the total effect is likely to have several components. The first component is proportional to the directional derivative of the effective electric field, along the stimulated axon $\frac{\partial E_l}{\partial l}$ and reflects the effects described by the cable equation [15]. The second component is proportional to the magnitude of the effective field E_l and mainly reveals itself at sharp bends and terminations of the axons. Finally, the third component may appear at the interface between white and gray matter due to a steep change in conductivity values [16].

The importance of considering local fiber orientations, for modeling TMS-induced effects, is indirectly supported by experimental studies, showing that changes in the orientation of the

E-mail address: SPKulikova@hse.ru.

https://doi.org/10.1016/j.softx.2020.100594

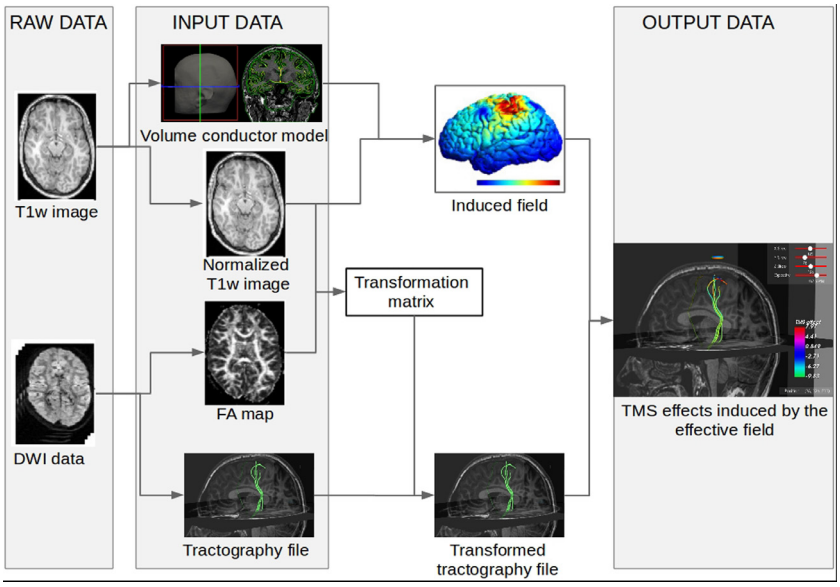

Fig. 1. Overview of the calculation pipeline showing the relationships between the input data, intermediate results and the output.

stimulating coil and, thus, in the orientation of the stimulated nervous fibers relative to the induced electric field, may have a significant impact on the observed TMS effects [17]. However, the current tools available for modeling TMS-effects, like SimNIBS [18], are restricted to the computation of the induced electric field within the brain tissues and do not allow evaluation of the described above theoretical models, which, to the best of our knowledge, still remain unconfirmed by experimental studies.

Thus, the goal of this work was to create a tool that incorporates information of the axonal orientation into the modeling of TMS-induced effects, according to the proposed theoretical mechanisms. Such a tool would allow researches to conduct experimental studies, relating the proposed theoretical mechanisms to the observed TMS effects, to improve our understanding of the neuronal mechanisms underlying TMS effects and to link them with behavioral data. Finally, considering individual characteristics of the white matter organization, during planning of the TMS sessions, should contribute to the development of personalized TMS-based therapeutic approaches.

The proposed tool can be viewed as an add-on to SimNIBS,[1] enriching its electric field modeling with analysis of the effective field, relative to individualized tractography data, derived from diffusion-weighted imaging (DWI). To take advantage of it, a user should provide 4 files. The first two files include a structural T1-weighted (T1w) image and a pre-computed volume conductor model of the head. These files are required to initiate and run SimNIBS simulation sessions. In addition, two files with DWI-derived data should be provided: a tractography dataset with streamlines, for which stimulation effects should be calculated and a fractional anisotropy map for co-registration purposes. Once the input data is provided and co-registered to each other, a user can select a position of the stimulating coil in an interactive window and initiate calculations. The results are visualized in a color-coded manner over the streamlines and saved for further analysis.

[1] https://simnibs.github.io/simnibs/build/html/index.html.

2. Software description

2.1. Software architecture

The general pipeline defining the relationships between the input data, intermediate results, outputs and the internal processes relating them is depicted on Fig. 1.

The input data includes four different files. To initiate and run SimNIBS simulation sessions, in order to model induced electric field, it is necessary to provide a structural T1w image (NifTI format [19]), and a corresponding, pre-computed volume conductor model (VCM) of the head. The VCM could be created from the T1w image, using either **mri2mesh** [20] or **headreco** [21] algorithms (for comparison see [18]). The two other input files contain DWI-derived data: a pre-computed fractional anisotropy map (NifTI format) and a tractography file (TRK format) containing streamlines that represent neuronal fibers for which stimulation effects should be calculated.

The first step is to bring all input data to the same reference space. To achieve this, affine transformation matrices are computed based on maximization of the mutual information between T1w and FA images. This procedure is performed in 4 steps and the resulting matrix at each step serves as a starting matrix for the optimization at the next step: (1) calculation of the center of mass transform; (2) calculation of a 3D translation transform; (3) calculation of a 3D rigid transform; (4) calculation of an affine transform. This stage takes around 15 min on an Intel Core i5 processor and should be performed only once per subject. Both optimization and subsequent data transformation rely on the algorithms implemented in DIPY (Diffusion Imaging in Python) [22].

Once the streamlines from the tractography file are transformed, their local directions, i.e. the tangent vectors $\vec{l}$, are calculated at each point. Then the transformed streamlines are visualized in 3D-space over the structural T1w image. The visualization part is implemented using the advanced interactive visualization tools from DIPY and FURY library. Within the opened Scene, the user can manually set the position of the stimulation coil (x, y, z) by clicking at a particular location within a horizontal section of the image. To select the desired level of the horizontal section, a 2D Line Slider can be used. Once the coil position is set, calculations of the TMS effects are triggered by a button click.

After initiation of the calculations, the following processes take place. First, a SimNIBS session is called to compute the induced electric field for the selected coil position (x, y, z) and the result is saved as a Gmsh mesh file. Calculation of the induced field takes less than 40 s. Then, for each point on each streamline, the effective field E_l and the associated TMS effects are calculated. To do that, first, one should get an electric field vector E at a given location. This vector is obtained by linear interpolation from the nodes of the tetrahedra that contains the point of interest. Once electric field is known at the point of interest, it is projected to the local direction of the streamline $\vec{l}$, to get the effective field E_l and to calculate its directional derivative, as a dot product between the gradient of the effective field E_l and the unit vector tangent to the streamline: $\frac{\partial E_l}{\partial l} = \nabla E_l \cdot \vec{l}$. Then, both components of the TMS-induced effects: $-\lambda E_l$ and $-\lambda^2 \frac{\partial E_l}{\partial l}$ (where λ is the length constant of the neural membrane equal to 2 mm), and their sum is saved in a txt file with **pickle.dump()** function for further analysis. Such calculations for one streamline with ∼1350 points take less than 10 s. Thus, generation of each figure in the Example section took less than 1 min. It is possible to speed up calculation by using parallel computing and neglecting deeply-localized points. However, these options are not available yet in the current version and, thus, it is recommended to run calculations only for the streamlines of interest extracted from the whole-brain tractography. Finally, the total TMS-induced effect is visualized over the streamlines in the Scene in a color-coded manner.

2.2. Software functionalities

The code was designed so that after providing the input data, a user could select, manually, a position of the stimulating coil in a 3D-Scene relative to the streamlines of interest and the structural T1w image. The selected position (x, y, z) is used as an input for **change_TMS_effects()** function, which is triggered by clicking on the calculation button. This function first calls **simulation()** function that runs SimNIBS simulation sessions. The **simulation()** function takes the selected coil position and the default simulation parameters (Magstim 70 mm Figure-of-Eight stimulation coil [23], the rate of current change within the stimulation coil $\frac{dI}{dt} = 10^6$ A/s). To change these parameters, one should modify the **ctmslist.fnamecoil** and **cpos.didt** within the **simulation()** function.

Then, the **get_field()** function gets the field vector at a given location (x, y, z). This is achieved by finding the closest tetrahedron containing the point (x, y, z) using a function **get_ttrd()**. To make this search efficient, the mesh structure is preprocessed using a **load_elem()** function which orders and indexes the mesh elements.

To get the directional derivatives of the effective field at a given point (x, y, z), **deriv_e_field()** function is called. This function relies on **get_field()** and **my_deriv()** functions (computes the 1st-order numerical derivative using a 3-point schema).

2.3. Sample code snippets

This section shows a code snippet for a **change_TMS_effect()** function that computes the TMS-related effects along the tractography streamlines (Listing 1). Once the mesh structure, containing the induced electric field, is preprocessed using a **load_elem()** function, the **change_TMS_effect()** function runs a nested loop over all points of all streamlines (elements of **new_streams_T1_array**). For each point **xyz** (numpy array), a **get_field()** is used, to get the electric field vector at that point **field_vector_xyz**. The first component of the TMS-induced effects, **effective_ field[stream][t,0]**, is obtained by projecting the field vector **field_vector_xyz** to the local direction of the streamline **streams_array_derivative[stream][t,:]** and multiplying by λ (**l1**). The second component of the TMS-induced effects, **effective_ field[stream][t,1]**, is computed my multiplying λ^2 (**l2**) and a directional derivative of the effective field which is computed by a **deriv_e_field()** function. Finally, **effective_field[stream][t,2]** contains the sum of the two TMS effects and the whole **effective_field** array is saved as a txt file.

```
def change_TMS_effects(x, y, z):
"""
Computes the TMS effects for a given coil position (x,y,z),
      according to the existing theoretical models, see Silva
      et al. (2008), elucidating the mechanisms and loci of
      neuronal excitation by transcranial magnetic
      stimulation, using a finite element model of a cortical
      sulcus
https://www.ncbi.nlm.nih.gov/pmc/articles/PMC2693370/
...
"""
  .....
  ttt = load_elems(field_mesh.nodes.node_coord,
      field_mesh.elm.node_number_list)

  effective_field = copy.deepcopy(new_streams_T1_array)

  for stream in range(len(new_streams_T1_array)):
    my_steam = copy.deepcopy(new_streams_T1_array[stream])
 print('starting ' + str(stream) + ' out of ' +
      str(len(new_streams_T1_array)))

    for t in range(len(my_steam[:, 0])):
      # -256/2 because of a freesurfer RAS coordinate system
      x = my_steam[t, 0] - 256 / 2
      y = my_steam[t, 1] - 256 / 2
      z = my_steam[t, 2] - 256 / 2
      xyz = np.asarray([x, y, z])

      field_vector_xyz = get_field(ttt, xyz, field_at_nodes)

      effective_field[stream][t, 0] = l1 *
     np.dot(field_vector_xyz,
     streams_array_derivative[stream][t, :])

      effective_field[stream][t, 1] = l2 * deriv_e_field(xyz,
     field_at_nodes, streams_array_derivative[stream][t, :],
     ttt)

      effective_field[stream][t, 2] =
     effective_field[stream][t, 0] +
     effective_field[stream][t, 1]

      if (effective_field[stream][t, 2] < effect_min):
        effect_min = effective_field[stream][t, 2]

      if effective_field[stream][t, 2] > effect_max:
        effect_max = effective_field[stream][t, 2]

    with open(current_out_dir + '/' + subject_name +
      '_effective_field.txt', 'wb') as f:
      pickle.dump(effective_field, f)
    f.close()
```

Listing 1: Code snippet for the **change_TMS_effect()** function that computes the TMS-related effects along the tractography streamlines

3. Illustrative example

This section demonstrates application of the proposed tool for calculation and visualization of the TMS-induced effects during stimulation of the cortico-spinal tract (CST). In this example we used MRI data from Novikov et al. [24], which was acquired on a 1.5T Siemens scanner (Siemens Healthcare, Erlangen, Germany) from a healthy adult male volunteer. A T1w image was acquired with a 1 mm isotropic spatial resolution, using a 3D fast gradient inversion recovery sequence (MPRage). The VCM file (subject.msh) and the normalized T1w image (T1fs_conform.nii.gz)

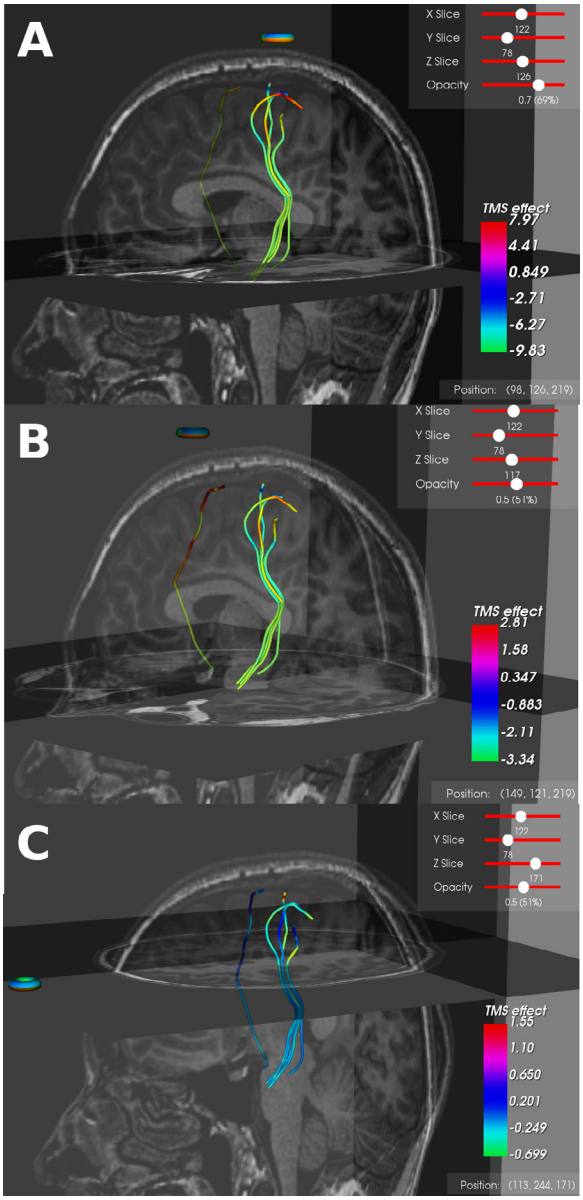

Fig. 2. Calculated effects for TMS of A. the left motor cortex; B. the right motor cortex and C. the frontal cortex (control stimulation site).

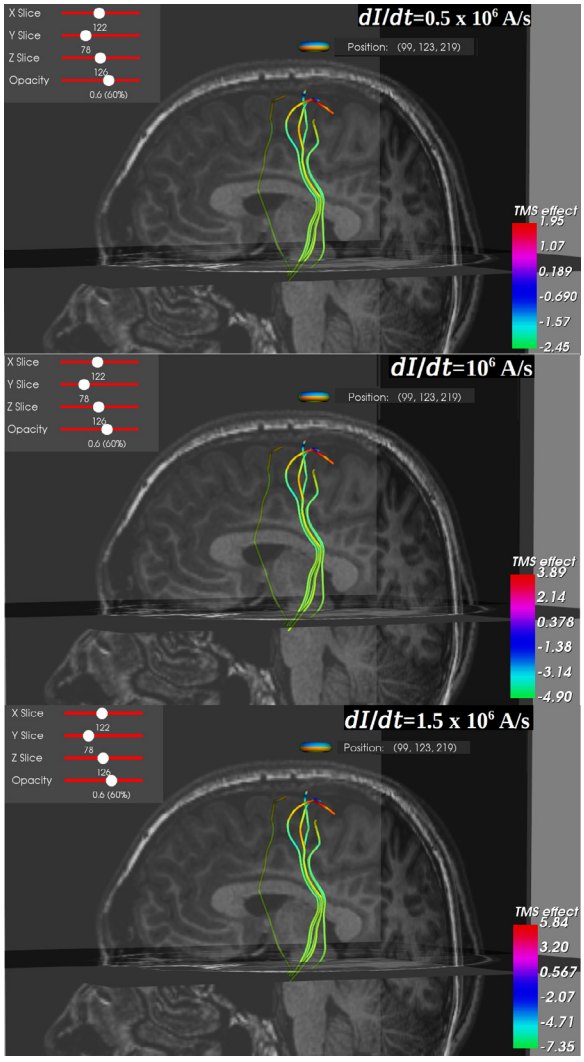

Fig. 3. Calculated TMS effects for the same coil position but for different rates of current change $\frac{dI}{dt}$.

were created from the raw T1w image using **mri2mesh**. Diffusion-weighted images were acquired using a DW-SE-EPI sequence with the following parameters: 64 diffusion gradient orientations (b = 1500 s/mm2), 4 b = 0 images, TE = 72 ms, TR = 14 s, parallel imaging GRAPPA factor 2, partial Fourier sampling factor 6/8. Diffusion data was pre-processed using Diffusion Toolkit (http://www.trackvis.org), a whole-brain tractography was performed according to a Q-ball model [25] and an FA map was calculated (dti_fa.nii). The resulting streamlines were visualized in TrackVis software (http://www.trackvis.org) and 6 typical streamlines from the CST (5 from left and 1 from right hemispheres, tracts.trk) were selected manually using the regions of interest in the primary motor area. The entire CST for that subject contained ∼1350 streamlines that could be processed in exactly the same way. However, for simplicity and visualization purposes this example was limited to a few representative streamlines.

To model stimulation of the CST, the coil was placed over the primary motor area. Thus, once the input files were prepared, loaded and co-registered to each other, we manually selected three positions of the coil to be tested: one above the CST streamlines in the left hemisphere, the second above the streamline from the right hemisphere, and one irrelevant control stimulation site over the frontal cortex. The resulting effects are depicted on Fig. 2.

As expected, the main effect of the stimulation of right and left hemispheres was localized on the streamlines from the same hemisphere, and stimulation at the frontal site had almost no impact on the considered streamlines. Furthermore, stimulation of the left hemisphere clearly demonstrates the effect of fiber geometry: even within closely located streamlines those bending in the vicinity of the stimulation site had much stronger stimulation effects. It could be also seen that increasing the rate of the current change $\frac{dI}{dt}$ while keeping all other stimulation settings the same produces similar patterns over the stimulated fibers, but with augmented TMS effects (Fig. 3).

However, in agreement with previous studies [17], changing only the coil orientation produced changes, both in the values of the TMS effects and in their pattern over the stimulated fibers (Fig. 4). Similarly, coil configuration also influenced both the values and the pattern of the TMS effects (Fig. 5).

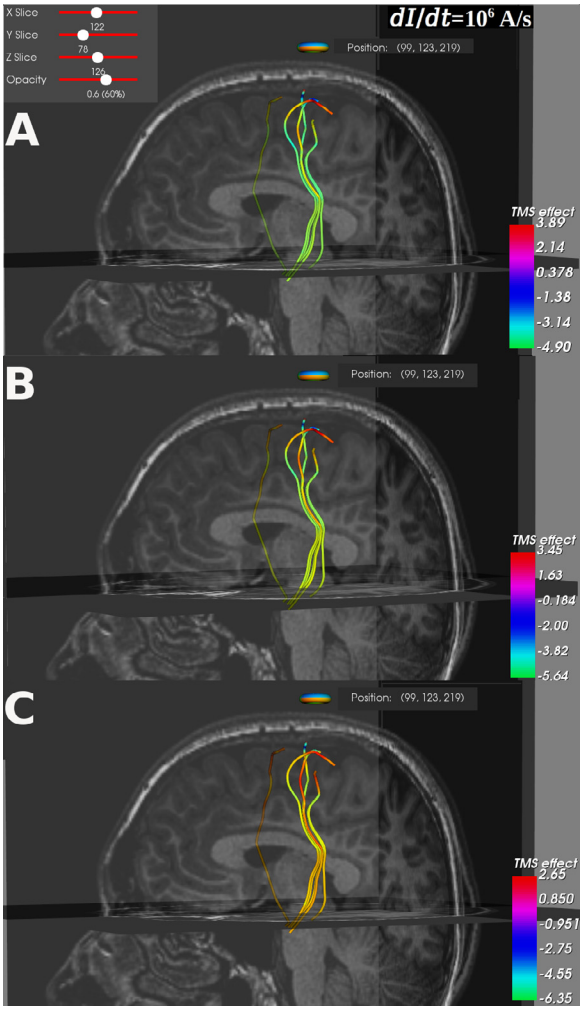

Fig. 4. Calculated TMS effects for the same coil position but for its different orientations: A. pointing posteriorly; B. pointing medially; C. pointing anteriorly. Orientation of the coil handle is not visualized in the current version.

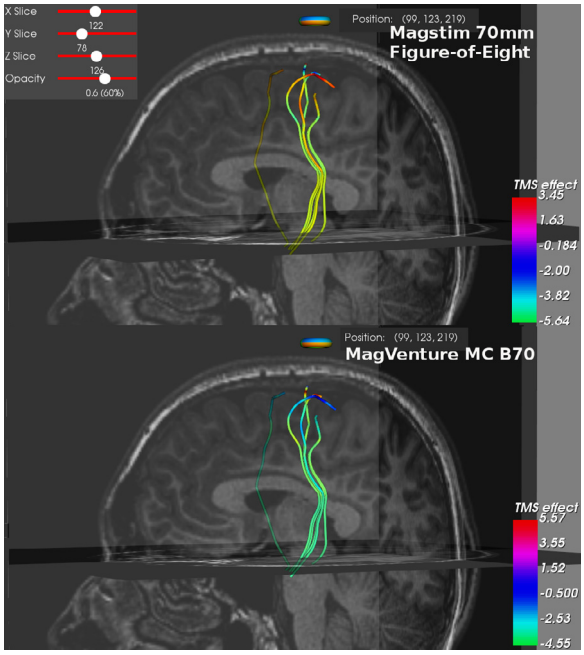

Fig. 5. Calculated TMS effects for two different coils: Magstim 70 mm Figure-of-Eight (up); Magstim 70 mm Figure-of-Eight (bottom). All other stimulation settings were kept the same.

4. Impact

Introducing a tool that allows calculating TMS-induced effects, while taking into account individual trajectories of the white matter fibers, should open new opportunities for studying neuronal mechanisms of the TMS. Joint analysis of the calculated TMS effects with the observed physiological responses (e.g. amplitudes of the motor evoked potentials for TMS of the motor cortex) should help to find the missing link between the existing theoretical models of TMS [13] and its experimentally observed effects. Enriching our understanding of the TMS mechanisms may bring new insights to TMS optimization and adaptive TMS mapping strategies. Existing approaches rely only on the induced electric field [26] and taking into account individual anatomical characteristics of the stimulated fibers may help to develop more efficient personalized approaches [27–29]: once paired in future with neuro-navigation, such approaches may help to optimize coil position and other stimulation settings with the reference to the individual form and position of the tracts of interest. Furthermore, since such optimization is totally computational, it will also help to reduce the duration of the TMS sessions, by reducing the time needed to localize the cortical area effectively stimulated by TMS and to adjust its settings.

However, much research is needed before any practical applications of such tract-based approaches become possible. First, it should be demonstrated that computed and experimentally-observed TMS effects are, indeed, related to each other [30]. Thus, it will be necessary to test the relationships between different stimulation metrics (i.e. maximal or mean stimulation effects, number of stimulated fibers, stimulation threshold, etc.) with the TMS effects observed at physiological or behavioral level. At this stage, statistical methods of subgroup analysis [31] may be applied, to reveal the subgroups of fibers that are the most responsive for a particular type of stimulation and that account for the observed effects. Such investigation is likely to be costly and time-consuming, since it requires acquisition and joint analysis of both TMS and MRI (T1w, DWI) data. It will be also important to pair the proposed approach with neuro-navigation. However, only after these steps, one may start developing approaches for optimization of the stimulation settings and verify whether tract-based optimization significantly enhances TMS effects and increases their predictability. Furthermore, it should be also kept in mind that TMS effects dramatically vary across different protocols (pulse intervals and total number of pulses) [3] meaning that it is necessary to extend current modeling of the TMS effects for a single pulse, to modeling of the effects produced by a sequence of pulses with custom defined parameters.

5. Conclusions

In this work, we have proposed a tool for interactive computation and visualization of the TMS-induced effects, at the individual white matter fiber trajectories derived from diffusion-weighted imaging. This tool could be used in future experimental TMS mapping studies to challenge the theoretical models of the TMS mechanisms with real experimental data, in an attempt to establish the links between the metrics describing axonal activation and the effects observed at the physiological and behavioral level. Other future improvements of the proposed tool will include (1) implementation of the subgroup discovery methods, for revealing subgroups of the white matter fibers that are the most responsive to a particular type of stimulations; (2) developing

optimization approaches, to identify the stimulation parameters maximizing the effect for a particular subset of white matter fibers; (3) pairing the proposed approach with neuro-navigation and (4) extending modeling of the TMS effects for different pulse sequences.

Declaration of competing interest

The authors declare that they have no known competing financial interests or personal relationships that could have appeared to influence the work reported in this paper.

Acknowledgments

This project was supported by Russian Science Foundation grant 18-75-00034. I would like to thank Dr. Maria Nazarova for providing example TMS and MRI data, Dr. Aleksey Buzmakov for the help with code testing and debugging and all instructors of the Neurohackademy 2019 who introduced to me many important tools to make this project possible.

References

[1] Iglesias A. Transcranial magnetic stimulation as treatment in multiple neurologic conditions.. Curr Neurol Neurosci Rep 2020;1(20). http://dx.doi.org/10.1007/s11910-020-1021-0.

[2] Terao Yasuo UY. Basic mechanisms of tms. J Clin Neurophysiol 2002;19(4):322–43.

[3] Ziemann U, Paulus W, Nitsche M, Pascual-Leone A, Byblow W, Berardelli A, Siebner H, Classen J, Cohen L, JC R. Consensus: Motor cortex plasticity protocols.. Brain Stimul 2008;1(3):164–82. http://dx.doi.org/10.1016/j.brs.2008.06.006.

[4] Huang Y-Z, Lu M-K, Antal A, Classen J, Nitsche M, Ziemann U, Ridding M, Hamada M, Ugawa Y, Jaberzadeh S, Suppa A, Paulus W, Rothwell J. Plasticity induced by non-invasive transcranial brain stimulation: A position paper. Clin Neurophysiol 2017;128(11):2318–29. http://dx.doi.org/10.1016/j.clinph.2017.09.007.

[5] Lopez-Alonso V, Cheeran B, Río-Rodríguez D, Fernández-Del-Olmo M. Inter-individual variability in response to non-invasive brain stimulation paradigms. Brain Stimul 2014;7(3):372—380. http://dx.doi.org/10.1016/j.brs.2014.02.004.

[6] Pellegrini M, Zoghi M, Jaberzadeh S. A checklist to reduce response variability in studies using transcranial magnetic stimulation for assessment of corticospinal excitability: A systematic review of the literature. Brain Connect 2020;10(2):53–71. http://dx.doi.org/10.1089/brain.2019.0715.

[7] Ovadia-Caro S, Khalil AA, Sehm B, Villringer A, Nikulin VV, Nazarova M. Predicting the response to non-invasive brain stimulation in stroke. Front Neurol 2019;10:302. http://dx.doi.org/10.3389/fneur.2019.00302.

[8] Zibman S, Pell GS, Barnea-Ygael N, Roth Y, Zangen A. Application of transcranial magnetic stimulation for major depression: coil design and neuroanatomical variability considerations. Eur Neuropsychopharmacol 2019. http://dx.doi.org/10.1016/j.euroneuro.2019.06.009.

[9] Syeda F, Magsood H, Lee EG, El-Gendy AA, Jiles DC, Hadimani RL. Effect of anatomical variability in brain on transcranial magnetic stimulation treatment. AIP Adv 2017;7(5):056711. http://dx.doi.org/10.1063/1.4974981.

[10] Hao WDZY, Liu ZM. Repetitive transcranial magnetic stimulation for improving function after stroke. Cochrane Database Syst Rev 2013;(5). http://dx.doi.org/10.1002/14651858.CD008862.pub2.

[11] O'Brien AT, Bertolucci F, Torrealba-Acosta G, Huerta R, Fregni F, Thibaut A. Non-invasive brain stimulation for fine motor improvement after stroke: a meta-analysis. Eur J Neurol 2018;25(8):1017–26. http://dx.doi.org/10.1111/ene.13643.

[12] Dougall M, Soares N, Weiser K, McDermott L, McIntosh A. Transcranial magnetic stimulation (TMS) for schizophrenia. Cochrane Database Syst Rev 2015;(8). http://dx.doi.org/10.1002/14651858.CD006081.pub2.

[13] Silva S, Basser PJ, Miranda PC. Elucidating the mechanisms and loci of neuronal excitation by transcranial magnetic stimulation using a finite element model of a cortical sulcus. Clin Neurophysiol 2008;119(10):2405–13. http://dx.doi.org/10.1016/j.clinph.2008.07.248.

[14] Geeter ND, Crevecoeur G, Leemans A, Dupré L. Effective electric fields along realistic DTI-based neural trajectories for modelling the stimulation mechanisms of TMS. Phys Med Biol 2014;60(2):453–71. http://dx.doi.org/10.1088/0031-9155/60/2/453.

[15] Roth BJ, Basser PJ. A model of the stimulation of a nerve fiber by electromagnetic induction. IEEE Trans Biomed Eng 1990;37(6):588–97. http://dx.doi.org/10.1109/10.55662.

[16] Miranda PC, Correia L, Salvador R, Basser PJ. Tissue heterogeneity as a mechanism for localized neural stimulation by applied electric fields. Phys Med Biol 2007;52(18):5603–17. http://dx.doi.org/10.1088/0031-9155/52/18/009.

[17] Richter L, Neumann G, Oung S, Schweikard A, Trillenberg P. Optimal coil orientation for transcranial magnetic stimulation. PLoS One 2013;8(4). http://dx.doi.org/10.1371/journal.pone.0060358.

[18] Saturnino GB, Madsen KH, Thielscher A. Electric field simulations for transcranial brain stimulation using FEM: an efficient implementation and error analysis. J Neural Eng 2019;16(6):066032. http://dx.doi.org/10.1088/1741-2552/ab41ba.

[19] Cox RH, Cox R, Ashburner J, Breman H, Fissell K, Haselgrove C, Holmes C, Lancaster J, Rex DE, Smith PAES, Woodward J, Cox R, Holmes C, Lancaster J, Smith S, Strother S, Smith SW. A (sort of) new image data format standard: Nifti-1. In: 10th annual meeting of the organization for human brain mapping. 2004.

[20] Windhoff M, Opitz A, Thielscher A. Electric field calculations in brain stimulation based on finite elements: An optimized processing pipeline for the generation and usage of accurate individual head models. Hum Brain Map 2013;34(4):923–35.

[21] Nielsen JD, Madsen KH, Puonti O, Siebner HR, Bauer C, Madsen CG, Saturnino GB, Thielscher A. Automatic skull segmentation from MR images for realistic volume conductor models of the head: Assessment of the state-of-the-art. NeuroImage 2018;174:587–98. http://dx.doi.org/10.1016/j.neuroimage.2018.03.001.

[22] Garyfallidis E, Brett M, Amirbekian B, Rokem A, van der Walt S, Descoteaux M, Nimmo-Smith I. Dipy, a library for the analysis of diffusion MRI data. Front Neuroinform 2014;8. http://dx.doi.org/10.3389/fninf.2014.00008.

[23] Thielscher A, Kammer T. Electric field properties of two commercial figure-8 coils in tms: calculation of focality and efficiency. Clin Neurophysiol 2004;115(7):1697–708. http://dx.doi.org/10.1016/j.clinph.2004.02.019.

[24] Novikov P, Nazarova M, Nikulin V. Tmsmap - software for quantitative analysis of TMS mapping results.. Front Hum Neurosci 2018;12(239). http://dx.doi.org/10.3389/fnhum.2018.00239.

[25] Descoteaux M, Angelino E, Fitzgibbons S, Deriche R. Regularized, fast, and robust analytical q-ball imaging. Magn Reson Med 2007;58(3):497–510. http://dx.doi.org/10.1002/mrm.21277.

[26] Weise K, Numssen O, Thielscher A, Hartwigsen G, Knsche TR. A novel approach to localize cortical TMS effects. NeuroImage 2020;209:116486. http://dx.doi.org/10.1016/j.neuroimage.2019.116486.

[27] Fox MD, Liu H, Pascual-Leone A. Identification of reproducible individualized targets for treatment of depression with TMS based on intrinsic connectivity. NeuroImage 2013;66:151–60. http://dx.doi.org/10.1016/j.neuroimage.2012.10.082.

[28] Tao Q, Yang Y, Yu H, Fan L, Luan S, Zhang L, Zhao H, Lv L, Jiang T, Song X. Anatomical connectivity-based strategy for targeting transcranial magnetic stimulation as antidepressant therapy. Front Psychiatry 2020;11:236. http://dx.doi.org/10.3389/fpsyt.2020.00236.

[29] Ahdab R, Ayache S, Brugires P, Goujon C, Lefaucheur J-P. Comparison of standard and navigated procedures of tms coil positioning over motor, premotor and prefrontal targets in patients with chronic pain and depression. Neurophysiol Clin/Clin Neurophysiol 2010;40(1):27–36. http://dx.doi.org/10.1016/j.neucli.2010.01.001.

[30] Buzmakov A, Kulikova S. Revealing relationships between tms-induced electric field in the brain tissues and the amplitude of the motor evoked potential.. In: Proc.: Internationl congress "neuroscience for medicine and psychology" Sudak, Crimea, Russia, October 6-16, 2020. 2020, p. 116. http://dx.doi.org/10.29003/m900.sudak.ns2020-16.

[31] Atzmueller M. Subgroup discovery. WIREs Data Min Knowl Discov 2015;5(1):35–49. http://dx.doi.org/10.1002/widm.1144.